CALT 68-2902

# Global CKM Fits with the Scan Method

Gerald Eigen,[1] Gregory Dubois-Felsmann,[2] David G. Hitlin,[3] and Frank C. Porter[3]

[1] *University of Bergen, 5007 Bergen, Norway*
[2] *SLAC National Accelerator Laboratory, Stanford, California 94309, USA*
[3] *California Institute of Technology, Pasadena, California 91125, USA*

We present results of a unitary triangle fit based on the scan method. This frequentist approach employs Gaussian uncertainties for experimental quantities, but makes no arbitrary assumptions about the distribution of theoretical errors. Instead, we perform a large number of fits, scanning over regions of plausible theory errors for each quantity, and retain those fits meeting a specific confidence level criterion, thereby constraining the $\bar{\rho}-\bar{\eta}$ plane using the standard input measurements (CKM matrix elements, $\sin 2\beta$, $B^0_{d,s}$ mixing, $\epsilon_K$) as well as branching fraction and *CP* asymmetry measurements of $B$ decays to $PP, PV, VV$, and $a_1 P$ final states to determine $\alpha$, $D^{(*)}K^{(*)}$ modes to determine $\gamma$, and $D^{(*)}\pi$ and $D\rho$ modes to determine $2\beta+\gamma$. We parameterize individual decay amplitudes in terms of color-allowed tree, color-suppressed tree, penguin, singlet penguin, electroweak penguin, as well as $W$-exchange and $W$-annihilation amplitudes. With this parameterization, we obtain a good fit to the measured branching fractions and *CP* asymmetries within the Standard Model *ansatz*, with no new physics contributions. This simultaneous fit allows us to determine the correlation between $\alpha$ and $\beta$ as well as between $\gamma$ and $\beta$.

PACS numbers: 12.15.Hh, 13.25.Hw, 14.65.Fy



## I. INTRODUCTION

The phase of the Cabibbo-Kobayashi-Maskawa (CKM) matrix [1] is responsible for *CP* violation in the Standard Model (SM). The unitarity relations within the CKM matrix provide an excellent laboratory to test this prediction, the relation ${V_{ub}}^* V_{ud} + {V_{cb}}^* V_{cd} + {V_{tb}}^* V_{td} = 0$ being particularly useful, since many measurements and theory inputs in the $B$ and $K$ systems can be combined for this test. Several such tests, such as those by the CKMfitter [2] and UT$_{fit}$ [3] groups are in common circulation. The former is a frequentist technique, the latter Bayesian. The scan method [4] presented herein takes a different approach in its treatment of the distribution of theoretical uncertainties.

We first describe the scan method. We then employ the method to extract CKM parameters using inputs standardized for the book *Physics of the B Factories* [5], comparing the results obtained with these parameters by CKMfitter and UT$_{fit}$, and investigating the question of consistency of the results with SM expectations. These fits utilize stand-alone determinations of the angle $\alpha$ and $\gamma$ as inputs. We then extend the scan method fit to include in the unitarity triangle parameter determination the measurements of $B$ decays to $PP, PV, VV$, and $a_1 P$ final states to determine $\alpha$, to $D^{(*)}K^{(*)}$ final states to determine $\gamma$, and to $D^{(*)}\pi$ and $D\rho$ final states to determine $2\beta+\gamma$. In this way, we are able for the first time to include the correlations between $\alpha$ and $\beta$ and $\gamma$ and $\beta$ in the extraction of the parameters of the unitarity triangle.

## II. FIT METHODOLOGY

The scan method is a frequentist-based fitting technique to determine the parameters of the CKM matrix. Rather than making assumptions as to the distribution of theory errors, it accounts for the uncertainties in the QCD parameters $f_{B_s}, f_{B_s}/f_{B_d}, B_{B_s}, B_{B_s}/B_{B_d}$, and $B_K$ and the CKM parameters $V_{ub}$ and $V_{cb}$ by scanning over the range of theory uncertainties using fixed grid or Monte Carlo (MC) methods. In the baseline fit, we combine measurements of $\Delta m_d, \Delta m_s, \epsilon_K, V_{cb}, V_{ub}, V_{ud}, V_{us}, \sin 2\beta, \alpha$ and $\gamma$ in the $\chi^2$ function:

$$\begin{aligned}\chi^2(\bar{\rho},\bar{\eta},p_i,t_j) = &\left(\frac{\langle\Delta m_{d,s}\rangle - \Delta m_{d,s}(\bar{\rho},\bar{\eta},p_i,t_j)}{\sigma_{\Delta m_{d,s}}}\right)^2 + \left(\frac{\langle|V_{cb,ub,ud,us}|\rangle - V_{cb,ub,ud,us}(\bar{\rho},\bar{\eta},p_i,t_j)}{\sigma_{V_{cb,ub,ud,us}}}\right)^2 \\ &+\left(\frac{\langle|\epsilon_K|\rangle - \epsilon_K(\bar{\rho},\bar{\eta},p_i,t_j)}{\sigma_{\epsilon_K}}\right)^2 + \left(\frac{\langle S_{\psi K^0}\rangle - \sin 2\beta(\bar{\rho},\bar{\eta},p_i)}{\sigma_{S_{\psi K^0}}}\right)^2 + \left(\frac{\langle\alpha\rangle - \alpha(\bar{\rho},\bar{\eta},p_i)}{\sigma_\alpha}\right)^2 \\ &+ \left(\frac{\langle\gamma\rangle - \gamma(\bar{\rho},\bar{\eta},p_i)}{\sigma_\gamma}\right)^2 + \sum\nolimits_k \left(\frac{\langle\mathcal{M}_k\rangle - \mathcal{M}_k(p_i)}{\sigma_{\mathcal{M}_k}}\right)^2 + \sum\nolimits_n \left(\frac{\langle\mathcal{T}_n\rangle - \mathcal{T}_n(p_i,t_j)}{\sigma_{\mathcal{T}_n}}\right)^2, \end{aligned} \quad (1)$$

where the $p_i$ are measured quantities including the Wolfenstein parameters [6] $A$ and $\lambda$, and the $t_j$ are QCD parameters. To account for correlations in the different

TABLE I. Observables used in the baseline fits. The first values of $V_{cb}$ and $V_{ub}$ are those used for the comparison with CKMfitter and UT$_{fit}$. The second, updated, values are those used in the scans over the theoretical quantities after separation of experimental and theory errors. The first values of $\alpha$ and $\gamma$ are those uses in the comparison with CKMfitter and UT$_{fit}$. The second values, obtained from our global fit, are used in the studies comparing the effect of the inclusion of $\mathcal{B}(B^+ \to \tau^+\nu)$.

| $m_t$ [GeV/c$^2$] | $m_c$ [GeV/c$^2$] | $\Delta m_d$ [ps$^{-1}$] | $\Delta m_s$ [ps$^{-1}$] |
|---|---|---|---|
| $173.3 \pm 0.9$ [13] | $1.275 \pm 0.025$ [13] | $0.507 \pm 0.004$ [13] | $17.7 \pm 0.08$ [13] |
| $V_{cb}$ | $V_{ub}$ | $V_{ud}$ | $V_{us}$ |
| $(4.06 \pm 0.13) \times 10^{-2}$ [20]<br>$(4.09 \pm 0.06 \pm 0.11) \times 10^{-2}$ [13] [a] | $(3.89 \pm 0.44) \times 10^{-3}$ [20]<br>$(4.15 \pm 0.31 \pm 0.48) \times 10^{-3}$ [13] [a] | $0.97425 \pm 0.0002$ [16] | $0.2208 \pm 0.0039$ [16] |
| $\epsilon_K$ | $\sin 2\beta$ | $\alpha$ | $\gamma$ |
| $(2.228 \pm 0.0011) \times 10^{-3}$ [13] | $0.0682 \pm 0.019$ [20] | $(90.0 \pm 5)^\circ$ [20]<br>$(84.0 \pm 2.1)^\circ$ [b] | $(76.0 \pm 10)^\circ$ [20]<br>$(78.8 \pm 4.4)^\circ$ [b] |

[a] experimental and theory errors separated
[b] Input from global fit (see below)

TABLE II. QCD parameters used in the baseline fits with "statistical" and theory uncertainties, respectively.

| $f_{B_s}$ [MeV] | $f_{B_s}/f_{B_d}$ | $B_{B_s}$ | $B_{B_s}/B_{B_d}$ | $B_K$ | Ref. |
|---|---|---|---|---|---|
| $250 \pm 5.4 \pm 11$ | $1.215 \pm 0.012 \pm 0.015$ | $1.33 \pm 0.06$ | $1.05 \pm 0.06$ | $0.737 \pm 0.006 \pm 0.020$ | [15] |
| $\eta_{cc}$ | $\eta_{ct}$ | $\eta_{tt}$ | $\eta_b$ | | |
| $1.39 \pm 0.35$ | $0.47 \pm 0.04$ | $0.5765 \pm 0.0065$ | $0.551 \pm 0.007$ | | [7] |

observables, we add terms in the $\chi^2$, denoted generically by $\mathcal{M}_k$, that include quark masses and $B$ meson masses.

We are careful to distinguish among different kinds of uncertainties. Observables with experimental errors only (statistical and systematic) are assumed to be Gaussian-distributed. Theoretical quantities such as lattice-derived QCD parameters, and inputs to $V_{ub}$ and $V_{cb}$, typically have two types of uncertainties. The first type of error is of a "statistical" nature, resulting from an input with statistical uncertainties or from Monte Carlo statistics in lattice calculations. We assume this error to be Gaussian-distributed and add corresponding terms to the $\chi^2$, denoted by $\mathcal{T}_n$. The second type of uncertainty is a theory error with no known underlying statistical distribution. We therefore make no assumption as to the distribution of these errors, and instead perform a scan over a large range of plausible values, doing a $\chi^2$ minimization at each point. The scan includes the QCD parameters ($f_{B_s}, f_{B_s}/f_{B_d}, B_{B_s}, B_{B_s}/B_{B_d}$ and $B_K$) and the CKM matrix elements $V_{ub}$ and $V_{cb}$. The QCD corrections $\eta_{cc}$, $\eta_{ct}$ and $\eta_{tt}$ used in the determination of $\epsilon_K$ and $\eta_b$ that appear in the prediction of $\Delta m_d$ also have theory errors. Although the fit methodology is able to scan over them, we do not do so, since this is unnecessary at the current level of precision. We parameterize $\eta_{cc}$ in terms of $m_c$ and $\alpha_s$ [7]. Tables I and II summarize the input parameters for our baseline fits. We are preparing a long article that includes a detailed discussion of all input values, provides a study of the correlations among the theory uncertainties and shows further results [8].

## III. COMPARISON TO CKMFITTER AND UT$_{fit}$

To begin, we compare the performance of the scan method with that of CKMfitter and UT$_{fit}$ using 19 input measurements ($V_{ud}$, $V_{us}$, $V_{cb}$, $V_{ub}$, $\epsilon_K, \Delta m_d, \Delta m_s, \sin 2\beta, \alpha, \gamma$, $f_{B_s}$, $B_{B_s}$, $f_{B_s}/f_{B_d}$, $B_{B_s}/B_{B_d}$, $B_K$, $m_t$, $m_c$, $m_{B_d}$, $m_{B_s}$), choosing values specified for the book *Physics of the B Factories* [5] to fit 13 parameters ($\bar{\rho}, \bar{\eta}, A, \lambda, f_{B_s}, B_{B_s}, f_{B_s}/f_{B_d}, B_{B_s}/B_{b_d}, B_K, m_t, m_c, m_{B_d}$, $m_{B_s}$). In these fits we use the central values and measurement errors for $\alpha$ and $\gamma$ in the $\chi^2$ function. We compute $\overline{m}_t(m_t)$, which enters into the Inami-Lim functions [12] for $\Delta m_d, \Delta m_s$ and $\epsilon_K$, in the $\overline{MS}$ scheme from the pole mass $m_t$ at three loop level for five quarks [9–11]. For fits having a $P(\chi^2)$ probability $> 32\%$, we plot $1\sigma$ contours in the $\bar{\rho} - \bar{\eta}$ plane. For the central value, we select the fit with the highest $P(\chi^2)$. We take the $\pm 1\sigma$ uncertainties from the maximum and minimum values of the envelope of all contours. We perform three different fits. In the first, we combine theory and experimental uncertainties, treating these as Gaussian. In the second, we scan over the theory uncertainties in $f_{B_s}, B_{B_s}, B_K$. In the third, we separate

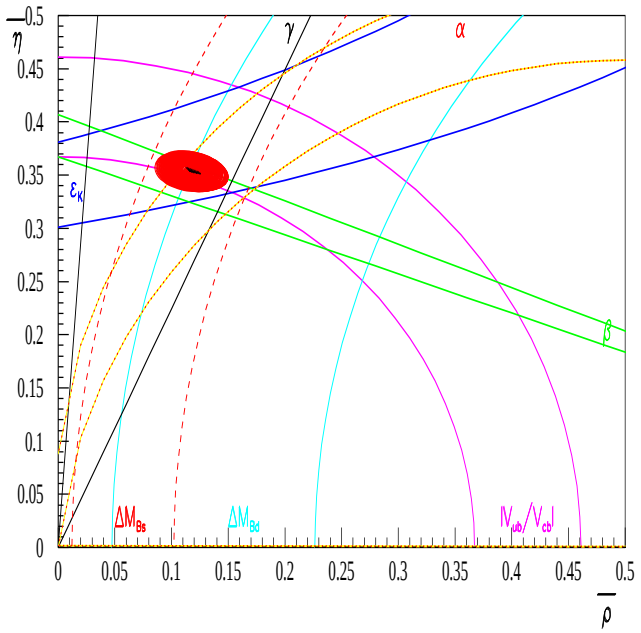


FIG. 1. Overlay of 68% CL contours in the $\bar{\rho} - \bar{\eta}$ plane for the inputs of *Physics of the B Factories* with scanning over $f_{B_s}, B_{B_s}$ and $B_K$.

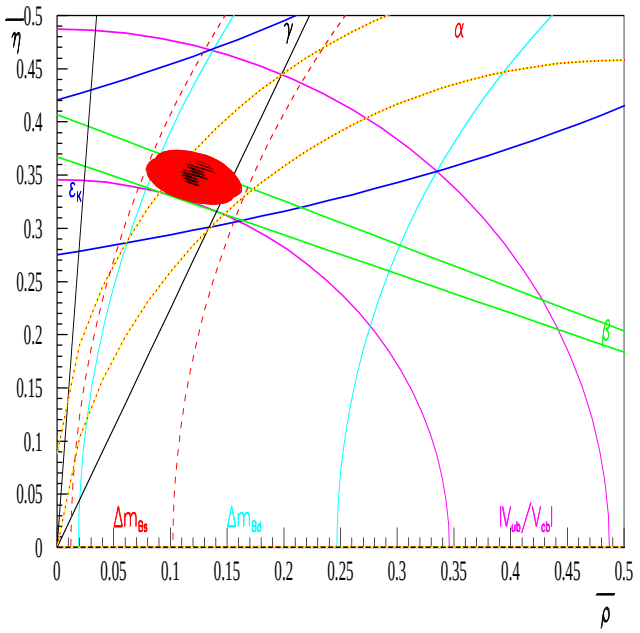


FIG. 2. Overlay of 68% CL contours in the $\bar{\rho} - \bar{\eta}$ plane for the inputs of *Physics of B the Factories* with scanning over $f_{B_s}, B_{B_s}, B_K, V_{ub}$ and $V_{cb}$.

TABLE III. Comparison of unitarity triangle parameters for different fitting techniques using inputs for *Physics of the B Factories*. The second and third columns show the results of fits by CKM fitter and UT$_{fit}$. The fourth column shows the result of the fit if no scanning over theory parameters is performed. The fifth column shows the fit results if we scan over the QCD parameters $f_{B_s}, f_{B_s}/f_{B_d}$ and $B_K$. The sixth column shows the fit result if we scan, in addition, over the theory errors associated with $V_{ub}$ and $V_{cb}$.

| Parameter | CKMfitter [5] | UT$_{fit}$ [5] | Our fit no scan | Scan method scan over $f_{B_s}, f_{B_s}/f_{B_d}, B_K$ | Scan method scan over $f_{B_s}, f_{B_s}/f_{B_d}, B_K, V_{cb}, V_{ub}$ |
|---|---|---|---|---|---|
| $\bar{\rho}$ | $0.121 \pm 0.02$ | $0.125 \pm 0.022$ | $0.119 \pm 0.013$ | $0.116^{+0.034}_{-0.031}$ | $0.130^{+0.030}_{-0.051}$ |
| $\bar{\eta}$ | $0.349 \pm 0.012$ | $0.347 \pm 0.014$ | $0.353 \pm 0.008$ | $0.353^{+0.020}_{-0.018}$ | $0.355^{+0.018}_{-0.032}$ |
| $\beta$ [°] | $21.7 \pm 1$ | $21.6 \pm 0.8$ | $21.9 \pm 0.3$ | $21.8^{+0.9}_{-0.9}$ | $22.2^{+0.4}_{-1.6}$ |
| $\alpha$ [°] | $87.5 \pm 3.2$ | $87.9 \pm 3.4$ | $86.8 \pm 2$ | $86.4^{+5.1}_{-4.6}$ | $87.9^{+6.3}_{-5.3}$ |
| $\gamma$ [°] | $70.9 \pm 3.2$ | $70.4 \pm 3.4$ | $71.4 \pm 2$ | $71.8^{+4.8}_{-5.1}$ | $69.8^{+7.4}_{-5.6}$ |

theory uncertainties from experimental uncertainties in $V_{ub}$ and $V_{cb}$ and scan over the former. Figure 1 shows the contours in the $\bar{\rho} - \bar{\eta}$ plane for the second fit and Fig. 2 shows those for the third fit, *i.e*, the most complete scan. Table III lists our results in comparison to those from CKMfitter and UT$_{fit}$. The three methods yield broadly similar results. Without scanning, the uncertainties in the unitarity triangle parameters are smaller than those from CKMfitter and UT$_{fit}$. Scanning only over the range of theory errors for the QCD parameters increases the uncertainties in the unitarity triangle parameters significantly. Scanning over $V_{ub}$ and $V_{cb}$ as well, the uncertainies are more than a factor of two larger than those from CKMfitter and UT$_{fit}$. The scan method finds acceptable fits in regions the other approaches do not explore, due to their assumptions as to the distribution of theory errors. This, of course, has an effect on the sensitivity of unitarity triangle fits to the contributions of physics beyond the SM. In view of the importance of searches for new physics in the flavor sector, it is worthwhile to use a procedure in making consistency tests of the unitarity triangle that treats the unknown statistical distribution of many theory errors with a minimum of assumptions. In this way claims of inconsistencies in unitarity triangle fits that violate the SM can be avoided.

We also perform fits with the PDG12 $V_{ub}$ and $V_{cb}$ averages [13] that are listed in Table I. Since the $V_{ub}$ and $V_{cb}$ results from exclusive modes are significantly lower than those from inclusive modes, the PDG uses scaling

factors on the total errors of 2.6 and 2.0, respectively. In order to use the scan method in this case, we separate the experimental and theory uncertainties. In all subsequent global fits of the CKM matrix, we scan over theory uncertainties in $V_{ub}, V_{cb}$, as well as those for $f_{B_s}$, $f_{B_s}/f_{B_d}$ and $B_K$. Figure 2 shows the overlay of 68% confidence level contours in the $\bar{\rho} - \bar{\eta}$ plane of all accepted fits.

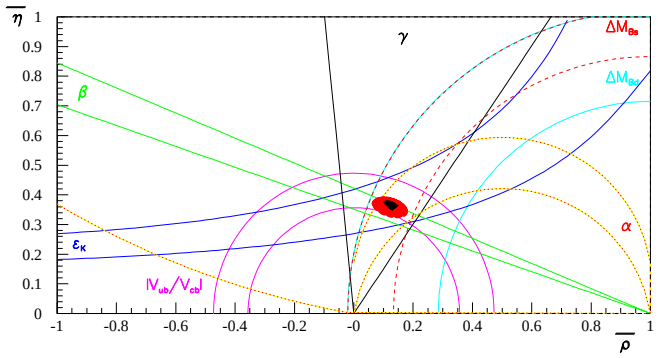


FIG. 3. Overlay of 95% CL contours in the $\bar{\rho} - \bar{\eta}$ plane for the baseline fit scan with 19 measurements without including $\mathcal{B}(B^+ \to \tau^+\nu)$.

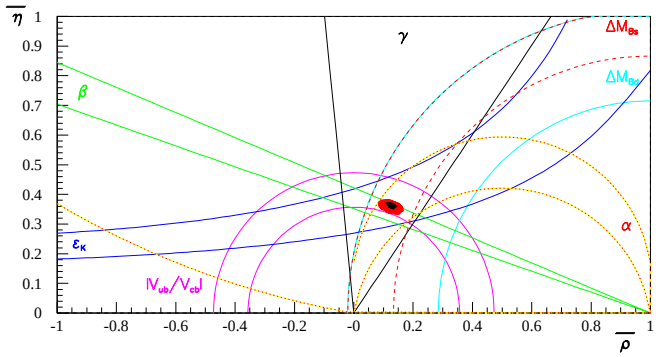


FIG. 4. Overlay of 95% CL contours in the $\bar{\rho} - \bar{\eta}$ plane for the baseline fit scan with 19 measurements with inclusion of $\mathcal{B}(B^+ \to \tau^+\nu)$.

## IV. RESULTS OF THE GLOBAL FITS

### A. Fit results with direct inputs of $\alpha$ and $\gamma$

To test the SM using the scan method, we relax the requirement for accepted fits to $P(\chi^2) > 5\%$. If we have any fits that meet this criterion, the SM is deemed to be compatible with the data at the present level of theoretical uncertainities. We form a contour corresponding to an accepted fit in any desired two-dimensional projection of parameter space. The contour consists of the boundary of the projection onto the plane of the multi-dimensional ellipsoid in parameter space satisfying $P(\chi^2) > 5\%$. We'll loosely refer to the contours as 95% CL contours. Taking the extrema of such a contour along a parameter axis provides a nominal 95% CL interval for the parameter. The procedure actually undercovers somewhat, in the limit of no theoretical uncertainties. However, the effect on coverage is not more than a few percent for the cases encountered here. Figure 3 shows the overlay of 95% CL contours in the $\bar{\rho} - \bar{\eta}$ plane for all accepted baseline fits using 19 measurements to fit 13 parameters, as in Section III. To obtain a range of values for a given parameter, we take the extrema of the union of the contours attached to accepted fits. Table IV shows the range of the unitarity triangle parameters thus obtained (hereinafter referred to as the 95% CL range).

The $B^+ \to \tau^+\nu$ branching fraction [17], measured by *BABAR* [18] and Belle [19], is very sensitive to contributions from a charged Higgs boson. The PDG average $\mathcal{B}(B^+ \to \tau^+\nu) = (1.66 \pm 0.33) \times 10^{-4}$ [13][20] is larger than the SM prediction of $\mathcal{B}(B^+ \to \tau^+\nu) = (1.2 \pm 0.25) \times 10^{-4}$ [21]. Figure 4 shows the results in the $\bar{\rho} - \bar{\eta}$ plane and Table IV summarizes the 95% CL ranges of unitarity parameters. Even with these high values of $\mathcal{B}(B^+ \to \tau^+\nu)$, we obtain a sizeable allowed $\bar{\rho} - \bar{\eta}$ region; there is no conflict with the SM. Belle has now presented a new measurement of $\mathcal{B}(B^+ \to \tau^+\nu) = (0.72^{+0.27}_{-0.25}(\text{stat}) \pm 0.11\ (\text{sys})) \times 10^{-4}$ [22] that reduces the world average, and in turn reduces any perceived conflict in the SM with the other measurements of the unitarity triangle.

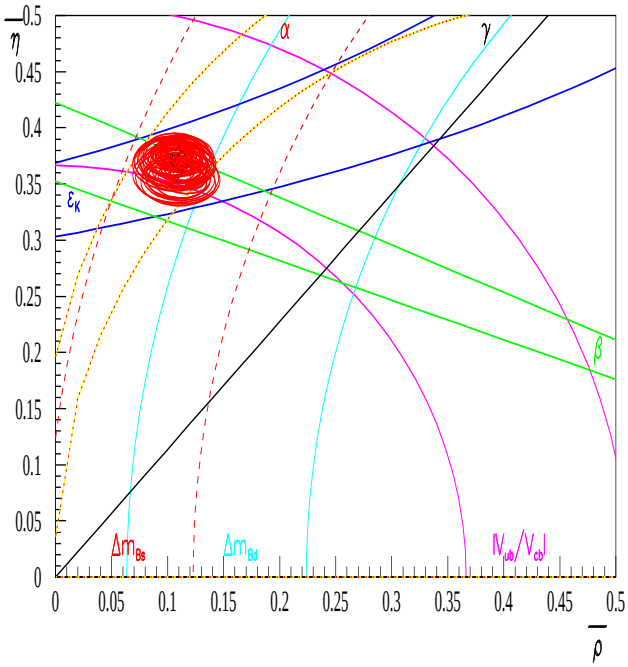


FIG. 5. Overlay of 95% CL contours in the $\bar{\rho} - \bar{\eta}$ plane for fits with 230 measurements without $\mathcal{B}(B^+ \to \tau^+\nu)$.

TABLE IV. The 95% CL ranges for unitarity triangle parameters from our baseline fit scans without and with the inclusion of $\mathcal{B}(B^+ \to \tau^+\nu)$. The values of $\alpha$ and $\gamma$ are, in these cases, computed from the values of $\bar{\rho}$ and $\bar{\eta}$.

| Parameter | $\bar{\rho}$ | $\bar{\eta}$ | $\beta$ [°] | $\alpha$ [°] | $\gamma$ [°] |
|---|---|---|---|---|---|
| Scan without $B^+ \to \tau^+\nu$ | $0.058 - 0.181$ | $0.324 - 0.395$ | $20.8 - 23.7$ | $77.1 - 95.9$ | $62.3 - 81.0$ |
| Scan with $B^+ \to \tau^+\nu$ | $0.085 - 0.159$ | $0.334 - 0.377$ | $21.2 - 22.9$ | $76.9 - 92.9$ | $65.2 - 76.9$ |

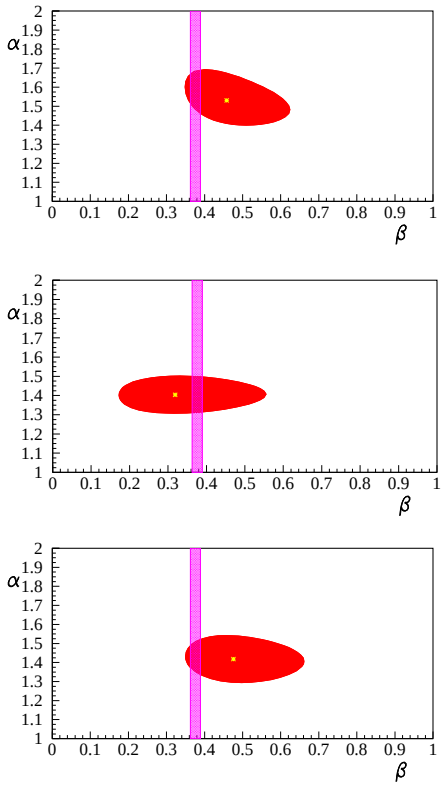


FIG. 6. Overlay of 95% CL contours in the $\alpha - \beta$ plane for $B \to PP$, $B \to PV$ and $B \to VV$ modes.

### B. Fit Results using Individual Measurements of Branching Fractions and *CP* Asymmetries of Various Decays

We also perform fits in which, instead of treating the values of $\alpha$ and $\gamma$ as inputs, we directly include the measurements that determine them. This allows us to determine the correlations in the extraction of the various unitarity triangle angles from the fit. We omit $\mathcal{B}(B^+ \to \tau^+\nu)$ in these fits; this has little effect on the results.

For the $\alpha$ determination, we include all measured branching fractions and *CP* asymmetries in $B \to PP$, $B \to PV$ and $B \to VV$ modes in the fit. Following the Gronau-Rosner approach [23], we parametrize amplitudes in terms of tree, color-suppressed tree, penguin, singlet penguin, $W$-annihilation/$W$-exchange, electroweak and color-suppressed electroweak diagrams (up to $\lambda^3$ beyond leading order). Thus for order $\lambda^3$, we consider SU(3) corrections for the tree, color-suppressed tree and penguin diagrams. Since calculations of branching fractions use the $B^+$ and $B^0_d$ life times, we add $\chi^2$ terms for them in the fit.

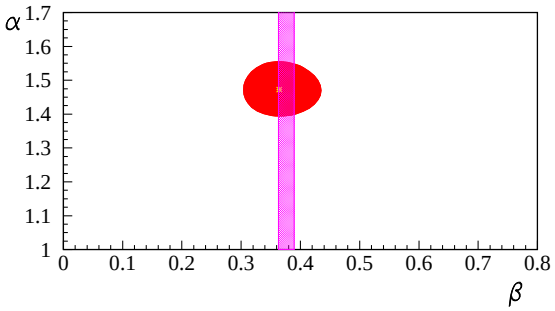


FIG. 7. Overlay of 95% CL contours in the $\alpha - \beta$ plane from fits including the $B \to PP$, $B \to PV$, $B \to VV$ and $B \to Pa_1$ modes. The vertical band shows the 68% CL range for $\beta$ obtained from $\sin 2\beta$ measurements [20].

For the $\gamma$ determination, we include measured branching fractions and *CP* asymmetries for $B^+ \to D^{(*)}K^+$ and $B^+ \to DK^{*+}$ decays analyzed in the Giri-Grossman-Soffer-Zupan (GGSZ) [24], Gronau-London-Wyler (GLW) [25] and Atwood-Dunietz-Soni (ADS) methods [26]. We also include branching fractions and *CP* asymmetries for $B^+ D^{(*)}\pi^+$ decays analyzed in the ADS method. Here, the observables are calculated in terms of $b \to c\bar{u}s(d)$ and $b \to u\bar{c}s(d)$ amplitudes. We also include time-dependent *CP* asymmetries in $B^0 \to D^{(*)+}\pi^-$ and $B^0 \to D^{(*)+}\rho^-$ decays that determine $\sin(2\beta + \gamma)$. Thus, the total number of measurements in the global fits increases to 230; the fit has 104 parameters. Figure 5 shows the 95% CL contours of all accepted fits in the $\bar{\rho} - \bar{\eta}$ plane. The allowed region is smaller than that for the baseline fits. Nonetheless, this result shows that the 230 measurements are in good agreement with the SM. This procedure accounts for possible correlations between $\alpha, \gamma$ and the other Wolfenstein parameters (*e.g.*, $\beta$).

## V. DETERMINATION OF $\alpha$ AND $\gamma$

In addition to the global fits of the CKM matrix, we perform separate fits that determine the unitarity triangles $\alpha$ and $\gamma$.

### A. Determination of $\alpha$

For the $\alpha$ determination we combine all measured branching fractions and *CP* asymmetries in $B \to PP$, $B \to PV$ and $B \to VV$ modes. We first perform separate fits for each class of decays. As in Section IV we parameterize the observables in terms of amplitudes, following the Gronau-Rosner method. We include $f_{B_s}$ and $f_{B_s}/f_{B_d}$ in the fit, but we do not scan over them, since these parameters appear only in the $W$-exchange and $W$-annihilation diagrams that are at order $\lambda^3$; any variation in these parameters is absorbed by adjusting the magnitude of the $W$-annihilation/$W$-exchange diagrams leaving $\alpha$ and the remaining parameters unchanged. We perform a single fit for each class of decays and plot 95% CL $\alpha - \beta$ contours. Figure 6 shows the $\alpha - \beta$ contours at 95% CL for the fits to $B \to PP, B \to PV$ and $B \to VV$ separately. The contours in the $\alpha - \beta$ plane, which are rather wide, encompass the world average $\beta = (21.4 \pm 0.8)^o$ measured using $b \to c\bar{c}s$ modes.

We next perform a combined fit of all measurements in $B \to PP, B \to PV$ and $B \to VV$ and $B \to Pa_1$ modes to extract $\alpha$. We use 181 measurements [20] to determine 94 parameters. Figure 7 shows the 95% CL contours in the $\alpha - \beta$ plane, which delineate a region that is considerably smaller than the contours of the fits for the individual decay classes. This is due to the fact that the $B \to PP$, $VV$ ($B \to PV$) modes yield larger (smaller) central values of $\beta$ than the $\sin 2\beta$ measurement in $b \to c\bar{c}s$ decays (see Table V). The fit probability is $P(\chi^2) = 9.6\%$. Table V lists all fit results for $\alpha$ and $\beta$. These results show that all measurements in $B \to PP, B \to PV$ and $B \to VV$ and $B \to Pa_1$ modes are consistent with the SM description and no new physics amplitudes are required.

### B. Determination of $\gamma$

For the $\gamma$ determination, we use branching fraction and *CP* asymmetries of $B^+ \to D^{(*)}K^+$ and $B^+ DK^{*+}$ decays analyzed in the GGSZ [24], GLW [25] and ADS [26] methods. We also include branching fractions and *CP* asymmetries of $B^+ \to D^{(*)}\pi^+$ decays analyzed in the ADS method and time-dependent *CP* asymmetries in $B^0 \to D^{(*)+}\pi^-$ and $B^0 \to D^{(*)+}\rho^-$ decays that determine $\sin(2\beta + \gamma)$. We separate the CKM factors, $|V_{us}V_{ub}^*|/|V_{cs}V_{cb}^*|$ and $|V_{ud}V_{ub}^*|/|V_{cd}V_{cb}^*|$ from the ratio of $b \to u$ to $b \to c$ amplitudes. We include the ratios $|V_{us}/V_{ud}|$ and $|V_{ub}/V_{cb}|$ in the fit, scanning over $|V_{ub}|$ and $|V_{cb}|$. Since the predictions contain a product of CKM factors and ratios of amplitudes, it is necessary to constrain the CKM factor in the fit to obtain sensible values for the amplitude ratios and CKM factors. We use 56 measurements [20] to extract 19 fit parameters, scanning over the constraint $|V_{ub}|/|V_{cb}|$. The probabilities for these fits range between $P(\chi^2) = 10.4\%$ and $P(\chi^2) = 14.4\%$. Figure 8 shows the resulting contours at 95% CL in the $\gamma - \beta$ plane. Table V lists the fit results. Again, these 56 modes are well-described within the SM and no new physics amplitudes are required.

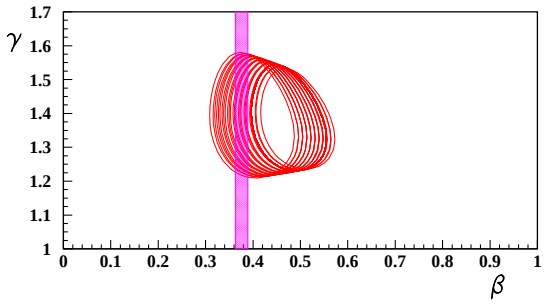


FIG. 8. Overlay of 95% CL contours in the $\gamma - \beta$ plane for fits including the $B \to DK^{(*)}, DK^*, D^{(*)}\pi, D\rho$ modes. The vertical band shows the 68% CL $\beta$ region obtained from $\sin 2\beta$ measurements [20].

## VI. CONCLUSION

The three fitting approaches: CKMfitter, UT$_{fit}$ and the scan method yield similar central values for $\bar{\rho}$ and $\bar{\eta}$ when presented with identical inputs. If we employ the scan method procedure of scanning over theory uncertainties in the QCD parameters, and $V_{ub}$ and $V_{cb}$ as well, making no assumption as to the distribution of theory errors, however, the allowed region in the $\bar{\rho} - \bar{\eta}$ plane is significantly larger. As a result, therefore, in the scan method measurements of the unitarity triangle provide good agreement with the SM; there is no need at this juncture to invoke new physics. The primary reason for the enlarged size of the allowed region in the $\bar{\rho} - \bar{\eta}$ plane is the large theory uncertainties in $V_{cb}$, $V_{ub}$ and the QCD parameters, coupled with the lack of knowledge about their distribution. As there is no principled frequentist method of ascertaining the distribution of theory errors, absent a Bayesian belief in the relevance of a Gaussian prior, the errors in $\bar{\rho}$ and $\bar{\eta}$ resulting from the scan method determination are obtained with a minimum of assumptions. They are thus less likely to result in spurious indications of a breakdown of the SM.

For this reason, using the scan method, we find no tension with the SM even when we include the current PDG value of $\mathcal{B}(B^+ \to \tau^+\nu) = (1.66 \pm 0.33) \times 10^{-4}$; the scan yields global fits consistent with the SM at 95% CL. When we include the recent Belle result as well, the allowed region becomes even larger. Using all measured branching fractions and *CP* asymmetries of $B \to PP$, $B \to PV$, $B \to VV$ modes and $B^+ \to D^{(*)}K^+, B \to DK^{*+}$ modes that are sensitive to $\alpha$ and $\gamma$, respectively, we see a reduced allowed region in the $\bar{\rho} - \bar{\eta}$ plane. From separate fits of branching fractions and *CP* asymmetries in these modes, we determine $\alpha - \beta$ and $\gamma - \beta$ contours. Though $\alpha$ measurements agree with each other and $\beta$ results are consistent with $\sin 2\beta$ from $b \to c\bar{c}s$ modes, the

TABLE V. Measurements of $\alpha$. $\beta$ and $\gamma$ from fits of branching fractions and $CP$ asymmetries in $B \to PP$, $B \to PV$, $B \to VV$ decays and in a combination of all modes combined plus $B \to Pa_1$ decays ($\alpha$) and $B \to D^{(*)}K(\pi) + B \to DK^*(\rho)$ decays ($\gamma$).

| | $B \to PP$ | $B \to PV$ | $B \to VV$ | $B$ modes combined | $B \to D^{(*)}K(\pi) + B \to DK^*(\rho)$ |
|---|---|---|---|---|---|
| $\alpha$ [°] | $86.5 \pm 3.4$ | $80.8 \pm 4.0$ | $81.4 \pm 5.2$ | $84^{+2.1}_{-2.0}$ | - |
| $\gamma$ [°] | - | - | - | - | $78.8^{+4.4}_{-4.2}$ |
| $\beta$ [°] | $25.8^{+4.0}_{-3.4}$ | $18.3^{+3.4}_{-2.9}$ | $27.5^{+7.4}_{-5.7}$ | $20.8^{+1.7}_{-1.5}$ | $22.8^{+7.8}_{-2.1}$ |

correlations among Wolfenstein parameters in the different measurements appear to be important. The values of $\alpha$, determined from a fit to all measured branching fractions and $CP$ asymmetries of $B \to PP$, $B \to PV$, $B \to VV$ and $B \to Pa_1$ modes, and $\gamma$, extracted from a fit to $B^+ \to D^{(*)}K^+, B \to DK^{*+}$, $B \to D^{(*)}\pi$ and $B^0 \to D^+\rho^-$ modes, agree with the SM expectations.


[1] N. Cabibbo, Phys. Rev. Lett. **10**, 531 (1963); M. Kobayashi and T. Maskawa, Prog. Th. Phys. **49**, 652 (1973).

[2] J. Charles *et al.*, Eur. Phys. Jour. **C41**, 1 (2005); updates at http://ckmfitter.in2p3.fr/.

[3] M. Bona *et al.*, JHEP **803**, 049 (2008); updates at http://www.utfit.org/.

[4] G. P. Dubois-Felsmann, G. Eigen, D. G. Hitlin and F. C. Porter, arXiv:hep-ph/0308262v2 (2003).

[5] Physics of the $B$ Factories, eds. A. Bevan *et al.*, Springer Verlag (2013).

[6] L. Wolfenstein, Phys. Rev. Lett. **51**, 1945 (1983).

[7] S. Herrlich and U. Nierste, Nucl. Phys. **B419**, 292, (1994); A.J. Buras, M. Jamin and P.H. Weisz, Nucl. Phys. **B347**, 491 (1990); S. Herrlich and U. Nierste, Phys. Rev. D **52**, 6505 (1995); Nucl. Phys. **B476**, 27 (1996).

[8] G. Eigen, G. P. Dubois-Felsmann, D. G. Hitlin and F. C. Porter, detailed article in preparation.

[9] K. Melnikov, T. van Ritbergen, Phys. Lett. **B482**, 99 (2000).

[10] N. Gray, D.J. Broadhurst, W. Grafe and K. Schilcher, Z. Phys. **C48**, 673 (1990).

[11] D.J. Broadhurst, N. Gray and K. Schilcher, Z. Phys. **C52**, 111 (1991).

[12] T. Inami and C. S. Lim, Prog. Th. Phys. 65, 297 (1981).

[13] J. Beringer *et al.* (Particle Data Group), Phys. Rev. **D86**, 010001 (2012).

[14] J. Laiho, E. Lunghi and R. S. Van de Water, Phys. Rev. **D81**, 034503 (2010). End of 2010 update: http://mypage.iu.edu/∼elunghi/webpage/LatAves/page7/page7.html

[15] J. Laiho, E. Lunghi and R. S. Van de Water, Phys. Rev. **D81**, 034503 (2010). End of 2011 update: http://mypage.iu.edu/∼elunghi/webpage/LatAves/page7/page7.html

[16] G. Colangelo *et al.*, Eur. Phys. J. **C71**, 1695 (2011).

[17] $CP$ conjugate states are implied.

[18] P. del Amo Sanchez *et al.*, Phys. Rev. **D81**, 051101 (2010); J.P. Lees *et al.*, arXiv:1207.0698 (2012).

[19] K. Hara *et al.*, Phys. Rev. **D.82**, 071101 (2010).

[20] D. Asner *et al.*, arXiv:1010.1589v3 (2011); www.slac.stanford.edu/xorg/hfag/triangle/index.html

[21] D. Silverman and H. Yao, Phys Rev. **D38**, 214 (1988).

[22] I. Adachi *et al.*, arXiv:1208.4678v2 (2012).

[23] M. Gronau, O. F. Hernandez, D. London and J.L. Rosner, Phys. Rev. **D50**, 4529 (1994); M. Gronau, D. Pirjol and T.M. Yan, Phys. Rev. **D60**, 034021 (1999); M. Gronau, D. Pirjol and T.M. Yan, Phys. Rev. **D69**, 119901(E) (2004); A.S. Dighe, M. Gronau and J.L. Rosner, Phys. Rev. **D57**, 1783 (1998); M. Gronau and J. L. Rosner, Phys. Rev. **D61**, 073008 (2000); M. Gronau, Phys. Rev. **D62**, 014031 (2000); A. Beneke *et al.*, Phys. Lett. **B638**, 68 (2006).

[24] A. Giri, Y. Grossman, A. Soffer and J. Zupan, Phys. Rev. **D68**, 054018 (2003).

[25] M. Gronau and D. London, Phys. Lett. **B253**, 483 (1991); M. Gronau and D. Wyler, Phys. Lett. **B265**, 172 (1991).

[26] D. Atwood, I. Dunietz, A. Soni, Phys. Rev. Lett. **78**, 3257 (1997); Phys. Rev. **D63**, 036005 (2001).